

# Influence of Global Mechanical Loading on Spatially Lithium Plating in Wound Lithium-Ion Batteries<sup>#</sup>

Ruohan Sun, Ying Chen\*, Haofeng Chen\*, Weiling Luan\*

School of Mechanical and Power Engineering, East China University of Science and Technology, Shanghai, 200237, China

(Corresponding Author: haofeng.chen@ecust.edu.cn ;luan@ecust.edu.cn)

## ABSTRACT

Lithium-ion batteries inevitably experience global mechanical loading during service, which significantly affects the electrode-separator interfacial contact, leading to spatial heterogeneity in current density and reaction overpotential. These effects can promote localized onset of lithium plating at the graphite anode, especially under low-temperature conditions. Lithium plating not only accelerates capacity fade and shortens cycle life, but the resultant dendrites may also pierce the separator, causing internal short circuits and potential safety hazards. In this work, using a wound NCM811/graphite pouch cell as a representative case, we combine numerical simulation with experimental characterization to systematically investigate the spatial heterogeneity of lithium plating on the graphite anode across different levels of global mechanical loading. The results reveal that global mechanical load preferentially compacts the wound region, significantly reducing separator porosity and electrolyte transport capability, thereby increasing ionic resistance and diffusion limitation. These findings elucidate the mechanical–electrochemical mechanisms governing lithium plating and provide a theoretical basis for optimizing cell structural design, stack-pressure strategies and the prevention of lithium-plating-induced safety risks in lithium-ion batteries.

**Keywords:** Lithium-ion batteries, lithium plating, mechanical load

## NONMENCLATURE

### Abbreviations

NCM	$\text{LiNi}_x\text{Co}_y\text{Mn}_z\text{O}_2$
NCM811	$\text{LiNi}_{0.8}\text{Co}_{0.1}\text{Mn}_{0.1}\text{O}_2$
SEM	Scanning Electron Microscope

### Symbols

$L$	Length of the straight segment( $\mu\text{m}$ )
$t$	Thickness of each layer( $\mu\text{m}$ )

$R_p$	Particle radius( $\mu\text{m}$ )
$\epsilon_s$	Volume fraction of the solid phase
$\epsilon_e$	Volume fraction of the liquid phase
$\sigma_s$	Solid phase conductivity( $\text{S}\cdot\text{m}^{-1}$ )
$\sigma_e$	Liquid phase conductivity( $\text{S}\cdot\text{m}^{-1}$ )
$D_e$	Liquid phase Li-diffusivity( $\text{m}^2\cdot\text{s}^{-1}$ )
$D_s$	Solid phase Li-diffusivity( $\text{m}^2\cdot\text{s}^{-1}$ )
$\nu$	Poisson's ratio
$E$	Young's modulus(MPa)

## 1. INTRODUCTION

Lithium-ion batteries are widely adopted as the primary power source for electric vehicles owing to their high energy density and long cycle life<sup>[1]</sup>. Nevertheless, performance degradation and safety issues remain great challenges for practical applications of batteries, among which lithium plating has recently attracted increasing attention<sup>[2]</sup>. Global mechanical loading can induce lithium deposition by changing the microstructure, interface contact state and lithium-ion transport kinetics of electrode materials. When the applied pressure is too low, the internal component contact is not sufficient, increasing the interface resistance, thereby promoting lithium plating<sup>[3]</sup>. In contrast, excessive pressure increases the internal stress, which may lead to irreversible lithium loss and further promote lithium plating. It is worth noting that under low temperature operation, the global mechanical load effect tends to intensify. At low temperature, the solid-phase Li diffusion rate in graphite and the liquid-phase Li diffusion rate in the electrolyte are significantly reduced<sup>[4]</sup>, which aggravates the deposition of lithium. Lithium plating can accelerate the performance degradation and endanger safety<sup>[5,6]</sup>. Although previous studies have preliminarily explored the effects of temperature and current density on lithium deposition, systematic research on how global mechanical loading affects the spatial inhomogeneity of

<sup>#</sup> This is a paper for the 17th International Conference on Applied Energy (ICAE2025), December 8-12, 2025, Bangkok, Thailand.

lithium deposition formation is still limited. Therefore, this study takes the wound NCM811/graphite lithium-ion battery as the representative research object, conducts different degrees of global mechanical load experiments, and observes the spatial inhomogeneity of lithium deposition on the graphite anode. In addition, a two-dimensional model with the wound structure is established to study the mechanism of spatial inhomogeneity in the process of lithium plating under global mechanical loading. These findings provide guidance for mechanical design and operation strategies to reduce the damage of lithium deposition in the wound lithium-ion batteries.

## 2. EXPERIMENTS AND NUMERICAL METHOD

### 2.1 Experimental analysis

The lithium-ion pouch cell used in this study is the ATL 854670(70 mm×46 mm×8.5 mm), with an NCM811/graphite material system. It has a nominal capacity of 3.7 Ah, a working voltage range of 3.2-4.25 V, and utilizes a LiPF<sub>6</sub> electrolyte.

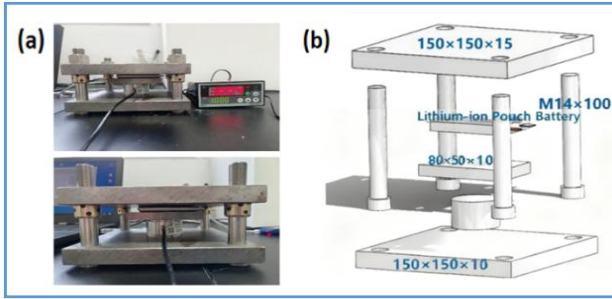


Fig. 1 (a) Physical image (b) schematic diagram of the global compression device.

After pre-cycling activation at a rate of 0.1 C within a voltage range of 2.8 V to 4.2 V, a global mechanical loading is applied using the compression device as shown in Fig.1. The device consists a three-layer aluminum frame: rigid upper and lower clamping plates and a middle precision positioning stage to secure the cell. The load is applied through four symmetrically arranged ball screw–nut assemblies with metric coarse thread with a nominal diameter of 10 mm. A torque wrench is used to provide continuous, stable axial pressure, ensuring uniform surface loading. Cyclic performance tests are then conducted on the battery under different levels of global mechanical load (0.3 MPa, 0.5 MPa) at 273.15 K.

### 2.2 Numerical method

A two-dimensional model is established, as shown in Fig.2, where the curved sections represent the wound region. From the inner to the outer side, the structure

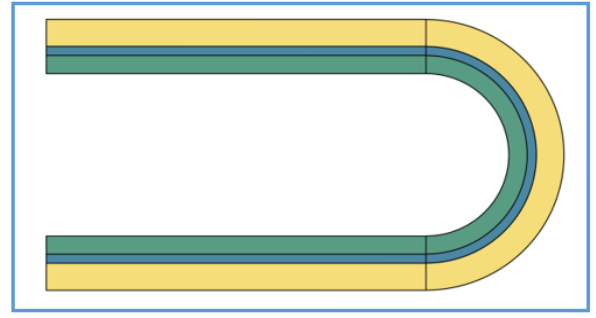


Fig. 2 Two-dimensional wound lithium-ion battery geometry

consists of the cathode, separator, and anode. The relevant parameters are provided in table 1. The (s) in the table represents the parameters for the straight-edge section, while (w) represents those for the wound region. The rationale for this piecewise definition will be explained in detail in the following section.

Table 1 Parameters of the model.

Parameters	Anode	Separator	Cathode
<b>Geometric</b>			
$L$	3000	3000	3000
$t^{[7]}$	53.4	10	40
$R_p^{[8]}$	6	/	6
$\epsilon_s^{[8]}$	0.6	0.5	0.6
$\epsilon_e^{[8]}$	0.4	0.5	0.34
<b>Transport</b>			
$\sigma_s^{[9]}$	10	/	1
$\sigma_e$	0.8(s)	0.8(s)	0.8(s)
	0.5(w)	0.5(w)	0.5(w)
$D_e$	10e-10(s)	10e-10(s)	10e-10(s)
	7e-11(w)	7e-11(w)	7e-11(w)
<b>Mechanical</b>			
$\nu$	0.32	0.4	0.25
$E$	120	75	150

To investigate the lithium deposition behavior at low temperatures, the temperature dependence is established using the Arrhenius equation<sup>[10]</sup> is presented below:

$$X(T) = X_{ref} \cdot \exp\left(\frac{E_a}{R} \left(\frac{1}{T_{ref}} - \frac{1}{T}\right)\right) \quad (1)$$

where  $X(T)$  is the temperature-dependent parameter, like  $D_s$ , reaction rate coefficient  $K$ ;  $T_{ref}$  is the reference temperature;  $X_{ref}$  is the reference value at  $T_{ref}$ ; and  $E_a$  is the activation energy.

In addition, the lithium deposition overpotential<sup>[9]</sup> can be expressed as follow:

$$\eta = \phi_s - \phi_e - E_{eq} \quad (2)$$

where  $E_{eq}$  is the equilibrium potential.

### 3. RESULTS AND DISCUSSION

#### 3.1 Spatial heterogeneity of lithium deposition induced by mechanical loading

At 273.15 K, different levels of global mechanical load (0.3 MPa, 0.5 MPa) are applied to NCM811 lithium-ion batteries. After the cycling, the batteries are disassembled, and the lithium plating on the anode is examined by scanning electron microscope. As shown in Fig.3, the application of global mechanical loading leads to uneven lithium deposition on the anode. Lithium plating preferentially occurs in the wound region of the anode, and the plating phenomenon becomes more obvious with increasing applied load.

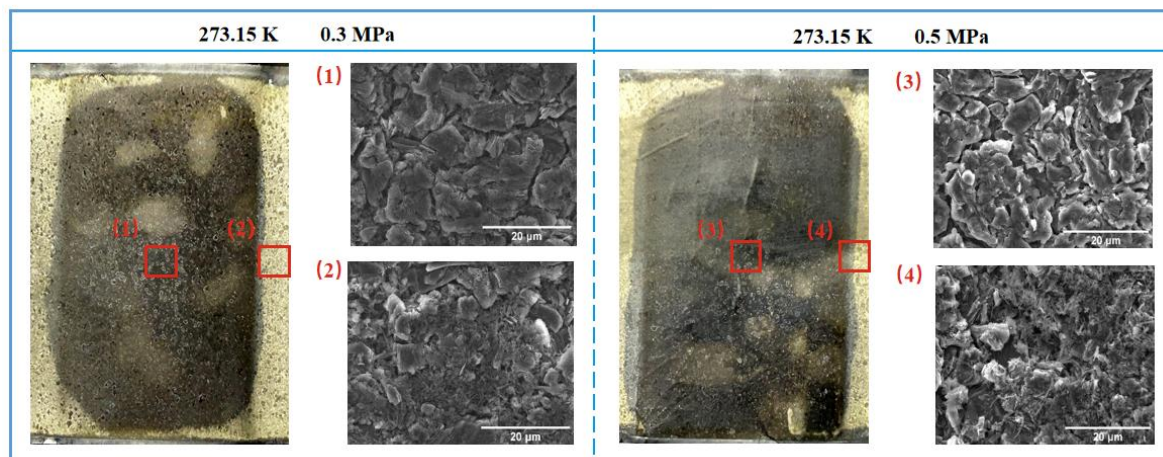


Fig. 3 Morphological image of the anode after disassembly and SEM characterization results.

#### 3.2 Pore closure in wound region restricting electrolyte transport

After applying a global mechanical load to the battery, as shown in Fig. 4, the compression in the wound section is significantly greater than that in the straight section. Due to the higher strain, the porosity of the separator in the wound area is notably reduced compared to the straight section<sup>[11]</sup>.

This porosity reduction affects electrolyte transport in two major ways: First, the available space for electrolyte flow becomes smaller, reducing the number of mobile ions in the electrolyte and the effective conduction pathways, which in turn increases the resistance to ion movement and decreases conductivity in the wound area. Second, the weakened flow of the electrolyte increases resistance to ion diffusion within the battery, thereby reducing the diffusion coefficient of the liquid phase.

Therefore, in the numerical model mentioned above,

the straight and wound sections are reasonably partitioned and assigned liquid-phase conductivity and liquid-phase diffusion coefficients, to capture the mechanically induced transport non-uniformity.

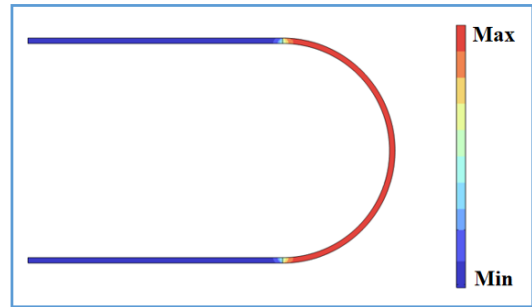


Fig. 4 Absolute value of volumetric strain after applying global mechanical load

#### 3.3 Transport limitations exacerbate polarization and induce spatially heterogeneous lithium plating

The decrease of ionic conductivity increases the ionic resistance of  $\text{Li}^+$  transport, while the decrease of diffusion coefficient slows down the mass transport of  $\text{Li}^+$  in the electrolyte filled pores. In summary, these transport limitations directly hinder the insertion kinetics of  $\text{Li}^+$  in porous electrodes. As shown in Fig.5 (a), the insertion of  $\text{Li}^+$  in wound area is slower than that in straight area. This kinetic limitation can lead to uneven distribution of current density, resulting in spatial variation.

As shown in Fig.5(b), the electrolyte concentration in the wound section is higher than that in the straight section. The elevated local concentration aggravates concentration polarization and limits the effective  $\text{Li}^+$  supply, thereby further hindering  $\text{Li}^+$  intercalation

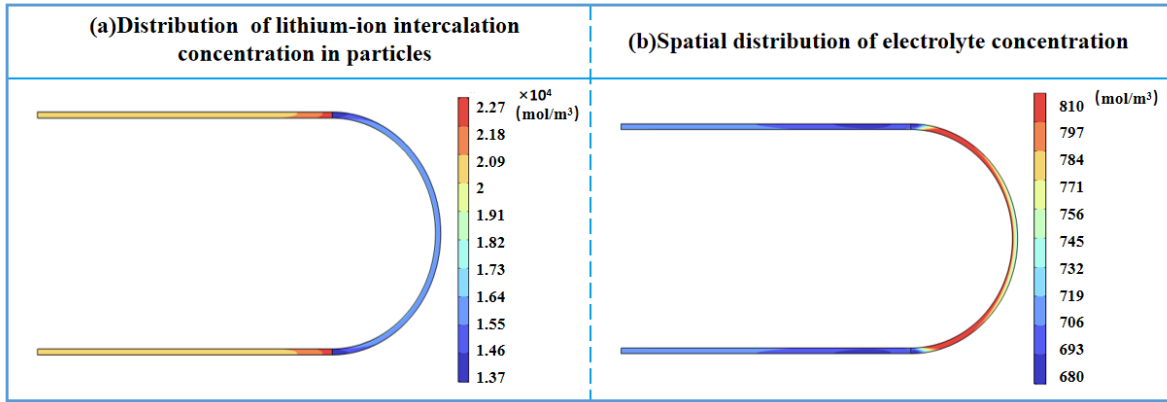


Fig. 5 Contour maps of (a) Lithium-ion insertion concentration (b) electrolyte concentration

kinetics. Meanwhile, the intensified polarization drives the local electrode potential to lower values and can reach the critical overpotential for lithium plating.

Once the local overpotential drops below the lithium-plating threshold,  $\text{Li}^+$  no longer preferentially intercalates into the active material; instead, it undergoes electrochemical reduction at the electrode surface and deposits as metallic lithium. As shown in Fig.6, the overpotential in the wound section drops below 0 V (vs.  $\text{Li}/\text{Li}^+$ ) earlier than in the straight section, which clearly suggests that lithium plating starts in this region first.

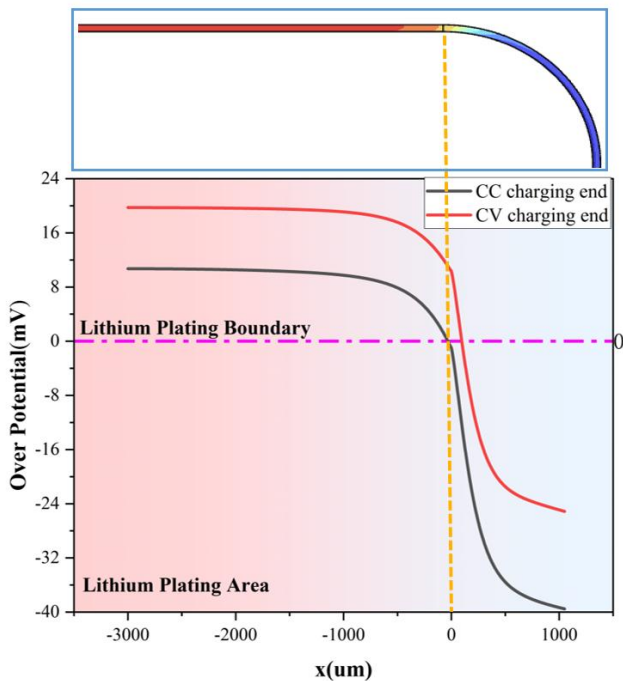


Fig. 6 Overpotential distribution diagram at the end of constant current and constant voltage charging.

#### 4. CONCLUSIONS

By combining numerical simulation and experimental verification, this study shows that the externally applied global compressive load plays a leading role in controlling the spatial evolution of lithium deposition on the graphite anode at low temperatures. The applied load preferentially compacts the wound area and reduces its porosity, thereby reducing the effective ionic conductivity and effective diffusion coefficient of the electrolyte. The decrease of these parameters aggravates the polarization and reduces the local overpotential, which is ultimately lower than the lithium plating threshold. This work provides a mechanistic insight into mechanically induced spatially inhomogeneous lithium deposition, and provides design criteria and operating boundaries for pressure-tolerant and low-temperature lithium-ion batteries.

#### ACKNOWLEDGEMENT

The authors gratefully acknowledge the support from the National Natural Science Foundation of China (52375144 and 52205153), the Shanghai Pujiang Program (23PJD019) and the Shanghai Gaofeng Project for University Academic Program Development.

#### REFERENCE

- [1] Tian Y, Lin C, Li HL, et al. Deep neural network-driven in situ detection and quantification of lithium plating on anodes in commercial lithium-ion batteries. *EcoMat* 2023;5(1):e12280. <https://doi.org/10.1002/eom2.12280>
- [2] Smith AJ, Fang Y, Mikheenkova A, et al. Localized lithium plating under mild cycling conditions in high-energy lithium-ion batteries. *Journal of Power Sources* 2023;573:233118. <https://doi.org/10.1016/j.jpowsour.2023.233118>
- [3] Daubinger P, Schelter M, Petersohn R, et al. Impact of

bracing on large format prismatic lithium-ion battery cells during aging. *Advanced Energy Materials* 2022;12(10):2102448.

<https://doi.org/10.1002/aenm.202102448>

[4] Laforgue A, Yuan XZ, Platt A, et al. Effects of fast charging at low temperature on a high energy Li-ion battery. *Journal of the Electrochemical Society* 2020;167(14):140521.

<https://doi.org/10.1149/1945-7111/abc4bc>

[5] You HZ, Jiang B, Zhu JG, et al. In-situ quantitative detection of irreversible lithium plating within full-lifespan of lithium-ion batteries. *Journal of Power Sources* 2023; 564:232892.

<https://doi.org/10.1016/j.jpowsour.2023.232892>

[6] You HZ, Wang XY, Zhu JG, et al. Investigation of lithium-ion battery nonlinear degradation by experiments and model-based simulation. *Energy Storage Materials* 2024;65:103083.

<https://doi.org/10.1016/j.ensm.2023.103083>

[7] Li J. Fundamental understanding of lithium plating in lithium-ion batteries: mechanism, model and mitigation strategies. Charlotte: University of North Carolina at Charlotte; 2024.

[8] Li Y, Shen Y, Wang X, et al. Electrochemical-thermal-mechanical coupling model considering lithium plating for multi-stage constant current fast charging of lithium-ion batteries. *CHAIN* 2025;2(2):148–63.

<https://doi.org/10.23919/chain.2025.000004>

[9] Cai J, Wei X, Wang X, et al. Revealing effects of pouch Li-ion battery structure on fast charging ability through numerical simulation. *Applied Energy* 2025;377:124438.

<https://doi.org/10.1016/j.apenergy.2024.124438>

[10] Hu X, Xu H, Ding C, et al. Numerical study on the thermal behavior of lithium-ion batteries based on an electrochemical–thermal coupling model. *Batteries* 2025;11(7):280.

<https://doi.org/10.3390/batteries11070280>

[11] Ai S, Xiao M, Chen J, et al. Microstructure Evolution of Lithium-Ion Battery Separator under Compressive Loading: In Situ Experiments and Image-Based Finite Simulations. *Energy Technology* 2022;10(6):2200017

<https://doi.org/10.1002/ente.202200017>